

Original Research

A Nude Mouse Model of Xenografted Hypertrophic Scar Cells to Test Therapeutics in the Skin

Bonnie C. Carney^{1,2,3,*}, Cynthia M. Simbulan-Rosenthal², Dean S. Rosenthal², Jeffrey W. Shupp^{1,2,3,4,5}

Academic Editor: Raffaele Serra

Submitted: 30 January 2024 Revised: 22 March 2024 Accepted: 16 April 2024 Published: 24 June 2024

Abstract

Background: Existing animal models for testing therapeutics in the skin are limited. Mouse and rat models lack similarity to human skin in structure and wound healing mechanism. Pigs are regarded as the best model with regards to similarity to human skin; however, these studies are expensive, time-consuming, and only small numbers of biologic replicates can be obtained. In addition, local-regional effects of treating wounds that are closely adjacent to one-another with different treatments make assessment of treatment effectiveness difficult in pig models. Therefore, here, a novel nude mouse model of xenografted porcine hypertrophic scar (HTS) cells was developed. This model system was developed to test if supplying hypo-pigmented cells with exogenous alpha melanocyte stimulating hormone (α -MSH) will reverse pigment loss in vivo. Methods: Dyschromic HTSs were created in red Duroc pigs. Epidermal scar cells (keratinocytes and melanocytes) were derived from regions of hyper-, hypo-, or normally pigmented scar or skin and were cryopreserved. Dermal fibroblasts (DFs) were isolated separately. Excisional wounds were created on nude mice and a grafting dome was placed. DFs were seeded on day 0 and formed a dermis. On day 3, epidermal cells were seeded onto the dermis. The grafting dome was removed on day 7 and hypo-pigmented xenografts were treated with synthetic α -MSH delivered with microneedling. On day 10, the xenografts were excised and saved. Sections were stained using hematoxylin and eosin hematoxylin and eosin (H&E) to assess xenograft structure. RNA was isolated and quantitative real-time polymerase chain reaction (qRT-PCR) was performed for melanogenesis-related genes TYR, TYRP1, and DCT. Results: The seeding of HTSDFs formed a dermis that is similar in structure and cellularity to HTS dermis from the porcine model. When hyper-, hypo-, and normally-pigmented epidermal cells were seeded, a fully stratified epithelium was formed by day 14. H&E staining and measurement of the epidermis showed the average thickness to be $0.11 \pm 0.07~\mu m$ vs. $0.06 \pm 0.03~\mu m$ in normal pig skin. Hypo-pigmented xenografts that were treated with synthetic α -MSH showed increases in pigmentation and had increased gene expression of TYR, TYRP1, and DCT compared to untreated controls (TYR: $2.7 \pm 1.1 \text{ vs. } 0.3 \pm 1.1; \text{ TYRP1: } 2.6 \pm 0.6 \text{ vs. } 0.3 \pm 0.7;$ DCT $0.7 \pm 0.9 \text{ vs. } 0.3 \pm 1$ -fold change from control; n = 3). Conclusions: The developed nude mouse skin xenograft model can be used to study treatments for the skin. The cells that can be xenografted can be derived from patient samples or from pig samples and form a robust dual-skin layer containing epidermis and dermis that is responsive to treatment. Specifically, we found that hypo-pigmented regions of scar can be stimulated to make melanin by synthetic α -MSH in vivo.

Keywords: hypertrophic scar; animal modek; burns; xenografts; dyschromia; melanocytes

1. Introduction

There is no perfect animal model for the study of hypertrophic scar (HTS) [1,2]. Studying patient samples is most likely the best recapitulation of the disease process; however, this strategy has the drawback that it is a snapshot in time. These samples do not provide information as to the natural history of HTS formation, as they must be taken after a scar is already formed. Additionally, HTS samples from patients are most likely at the severe end of the spectrum because samples large enough to graft can most often only be collected from severe HTS that requires excision. Murine species are generally not accepted as models of HTS because of the "loose-skinned" nature of these animals [3].

They also have a panniculus carnosus which allows them to heal by contraction instead of by granulation tissue deposition and re-epithelialization. As such, murine species that are not transgenic do not form robust fibroproliferative HTS.

Non-animal models for wound healing and scar formation have also been suggested [4]. These include *in vitro* models utilizing co-cultures of HTS-derived cells and organotypic culturing of biopsies of HTS. *Ex vivo* models utilizing excised human skin have also been proposed. While these models are useful for certain research questions, the drawback of not having the full *in vivo* system is clear.

¹Firefighters' Burn and Surgical Research Laboratory, MedStar Health Research Institute, Washington, D.C. 20010, USA

²Department of Biochemistry and Molecular & Cellular Biology, Georgetown University School of Medicine, Washington, D.C. 20007, USA

 $^{^3}$ Department of Surgery, Georgetown University School of Medicine, Washington, D.C. 20007, USA

⁴The Burn Center, Department of Surgery, MedStar Washington Hospital Center, Washington, D.C. 20010, USA

⁵Department of Plastic and Reconstructive Surgery, Georgetown University School of Medicine, Washington, D.C. 20007, USA

^{*}Correspondence: bonnie.c.carney@medstar.net (Bonnie C. Carney)

Nude mouse models of xenografted normal human skin have been used to create human-like HTS [5–7]. Although the skin was normal, and not HTS when it was xenografted, the skin forms scar that has many of the morphologic and histologic criteria of HTS. Additional models have been developed where the normal skin is "scratched" to create a wound in the skin that then forms additional HTS [8]. While these models are useful, and they have shown retention of the HTS and pigmentation phenotype even 1-year post-xenografting, the etiology of HTS is not the same as the etiology of full thickness wounding or burn injury. Lastly, this model relies on the availability of large amounts of normal human skin, a resource that is not universally available.

In prior work, it was shown that hypo-pigmented melanocytes derived from human hypopigmented hypertrophic scars could be stimulated by synthetic alpha melanocyte stimulating hormone (NDP α -MSH) to produce melanin in vitro [9]. The next step was to move from in vitro work with cells only to an in vivo animal model. Ideally, treatments for hypo-pigmentation would have been tested directly in the most similar model to the human phenotype. Models of HTS are resource-intensive and can be difficult to work with, as they utilize pigs as a model system and require many animals for the creation of just a few individual scars. Thus, if "pseudo" HTSs can be created on the back of athymic mice, multiple different treatments can be tested to optimize methods with larger sample sizes. Further, cells from areas with different pigmentation phenotypes can be isolated and studied independently without effects from their neighboring differentially pigmented scar areas. The reason for xenografting the scar cells onto athymic mouse wound beds is to allow for the support of the fully functioning dermal/subdermal system of the mouse to provide vascularization and structure to support the cells. The cells will then form a more translatable stratified skin and the xenografted "scars" can be studied intact, as opposed to cells in culture, which may not behave identically to those in vivo.

There is no previously optimized dose for NDP α -MSH that could be used *in vivo*. Previous testing in healthy volunteers, vitiligo patients, and erythropoietic protoporphyria (EPP) patients have used either a subcutaneous dose in initial studies [10–13], or a systemic slow-release dermal implant in later studies [14–18]. These systemic techniques for drug delivery are not ideal for the treatment of hypopigmentation in HTS because they would result in further dyspigmentation in normal skin and hyper-pigmented scar. Instead, a topical, scar targeted approach was desired. Synthetic α -MSH has minimal ability to penetrate the epidermis and does not induce pigmentation after topical application [19,20]. Therefore, a method for drug delivery based on a new concept in HTS treatment where ablative fractional lasers are used as a drug delivery enhancement technique was used [21–24]. Ablative fractional lasers (AFL)

produce microchannels in the skin or scar at pre-determined depths in a symmetrical pattern. The drugs can then be delivered topically and penetrate the epidermis and dermis depending on the depth of the channel. Due to logistic and cost constraints of working with the AFL, a microneedling technique for drug delivery was chosen which creates similar channels in skin and scar and allows for topical application following channel creation [25–27].

Nude mice are ideal for xenografting because they lack an immune system, and hence, do not reject the cells when grafted [28]. A xenograft model that has been used extensively in our lab in prior experiments was modified for use in the current experiment. This model has been used previously to create human skin xenografts with primary human fibroblasts and immortalized primary human keratinocytes derived from neonatal foreskin. In this prior work, the effect of sulfur mustard on the death receptor pathway and apoptotic processes was studied in human xenografts [29]. Another project studied the dysregulation of inhibitor of DNA binding 2 (Id2) in relation to the regulation of genetically modified keratinocytes [30]. The model has also been used to create xenografts from freshly isolated, cultured, or genetically modified human cell lines in work from multiple other groups [31]. These groups have studied a number of epidermal tumor cell lines, as well as freshly isolated cells from neonates. Lastly, this model has been used to study melanoma cells [32].

The work reported here is novel because the cells of interest were derived from adult pigs, not neonates. Previously reported upon use of the model relied exclusively on neonatal-derived, genetically immortalized, or cancer cell lines. The modified model was first developed with normally pigmented cells derived from un-injured skin. Then, the hypothesis that synthetic α -MSH could be used as a treatment for hypo-pigmentation was tested in hypopigmented xenografts *in vivo*.

2. Materials and Methods

2.1 Creation of Dyschromic HTS in Red Duroc Pigs as the Source of Cells for Xenografting

All animal work described was reviewed and approved by the MedStar Health Research Institute's Institutional Animal Care and Use Committee (IACUC). Juvenile castrated male red Duroc swine (30–55 kg) were received and handled according to facility standard operating procedures under an animal care and use program accredited by the Association for Assessment and Accreditation of Laboratory Animal Care International and the Public Health Service.

On the day of surgery, animals (n = 3) were anesthetized with a combination of ketamine (10 mg/kg) and xylazine (2 mg/kg) that were delivered intramuscularly. Animals were intubated, maintained on isoflurane, placed on a warming blanket, and ventilated while heart rate, blood pressure, peripheral oxygen saturation, end-tidal carbon



dioxide saturation, and core body temperature were continuously monitored. The body hair was clipped, and the skin was prepped with chlorhexidine gluconate scrub.

To create full-thickness wounds, one $10.16 \text{ cm} \times 10.16 \text{ cm}$ (4-inch \times 4 inch) square was excised over the rib cage on each side of the animal, at a total dermatome setting of 0.090 inches (0.030 in which is the maximum dermatome setting \times 3 passes) using a dermatome (Zimmer, Ltd., Swindon, UK) as previously described [33–35]. A Goulian blade was then used to ensure that the entire square was wounded down to full thickness.

The nature of the excisional wounding procedure creates wounds that are down to the subcutaneous fat and removes all viable dermal elements, including hair follicles and shafts, and apocrine tissues. Mepilex® Ag dressings (Molnlycke, Gothenburg, Sweden) were applied after wound creation and at each dressing change. Animals were fitted with custom-made neoprene vests [36], which completely covered the applied dressings while still allowing mobility of the animal. Buprenorphine (0.005 mg/kg) and fentanyl (25 mcg/hour) were administered for pain control at the end of each surgical procedure. Each week, through 133 days, animals underwent wound cleansing, imaging, biopsy procurement, dressing changes, and vest replacement. The animals were examined at least twice daily to monitor animal health and to identify any signs of pain, wound infection, or distress, of which there were no serious events.

2.2 Culturing Primary Cell Lines

2.2.1 Pig HTS Epidermal Cells Consisting of Melanocytes and Keratinocytes

On day 134 post-injury, porcine HTS was excised, split into distinct regions of hyper- and hypo-pigmented scar, cut into thin 0.5 cm strips, and processed with $1 \times$ dispase solution (CellnTec, Bern, Switzerland) within 1 hour of excision from n = 3 animals. Epidermal sheets were peeled from the dermis and epidermal cells, consisting of melanocytes and keratinocytes, were isolated from regions of hyper-, hypo-, or normal pigmentation as described previously [37] (Fig. 1). Briefly, single cells were mechanically disaggregated by serological pipetting 25 times. The resulting cell suspension was filtered through a 70 µm filter, cells were pelleted at 600 g for 5 minutes. The cells were cryopreserved in 90% FBS and 10% DMSO using a cryochamber (Corning, Corning, NY, USA) at an approximate rate of -1 °C/min and were subsequently stored in LN2 until thawing and use in the xenograft model. One 4 inch by 4-inch HTS on a duroc pig resulted in enough cells to create ~12 nude mouse xenografts (6 hypo- and 6 hyper-pigmented) depending on the percentage of the different pigmentation phenotypes in each of the scars.

2.2.2 Pig HTS and Normal Dermal Fibroblasts

In hyper-, hypo-, and normally-pigmented skin and scar, after the epidermal sheets were peeled, the dermal

pieces were further processed with 1 mg/mL collagenase (MP Biomedicals, Solon, OH, USA) at 37 °C for 4 hours to obtain fibroblasts. The resulting cell suspension was raised to a volume of 40 mL with PBS and was shaken vigorously to release single cells. The final suspension was then passed through a 45-μm filter. The single cell suspension was spun at 600 g for 5 minutes, and the resulting cell suspension was reconstituted and seeded at a density of 4000 cells/cm². Nonadherent cells were washed away after 24 hours, and the cells were then grown and subcultured at 37 °C and 5% CO₂ in the media detailed previously. Fibroblast cells were cryopreserved in freezing media containing 80% complete media, 10% FBS, and 10% DMSO using a cryochamber (Corning) at an approximate rate of −1 °C/min and were subsequently stored in LN2 until thawing.

2.3 Animal Model

2.3.1 3D Printing of Domes

The company that manufactured the domes in previous literature is now out of business and there is no current manufacturer [31,32]. As such, domes were 3D printed as a substitute. Domes were designed using Blender (Blender Foundation, Amsterdam, Netherlands) version 2.79. Ultimaker software version 3.6.0 was used for slicing (Cura, Geldermalsen, Netherlands). eSUN eLastic TPE 85A 1.75 mm Flexible 3D printer filament in natural white was used as the material (INTSERVO, Cary, NC, USA). Domes were 3D printed using a Qidi (Ruian, China) X-one 3D printer with a 400 μm nozzle at 212 °C on a heated print bed at 95 °C. The diameter of the hole in the flange was 1 cm. A 2 mm biopsy punch was used to create a hole in the top of the dome to allow for evaporation of cell media. Domes were sterilized in the autoclave at 105 °C, just below the melting temperature of the material.

2.3.2. Dome Placement and Fibroblast Cell Seeding

NCr-Foxn1nu mice (Charles River Laboratories, Wilmington, MA, USA) at an age of 5-8 weeks were used. All animal procedures were conducted in a laminar flow hood with sterile materials. On the day of cell seeding (day 0), anesthesia was induced by 5% isoflurane in an induction box. After an appropriate plane of anesthesia was reached, the animal was transferred to a nose cone and maintained on 3.5% isoflurane for the remainder of the experiment. The skin was surgically prepped using Chloraprep (Becton Dickinson, Franklin Lakes, NJ, USA). A 1 cm in diameter full thickness circular excisional wound was created using curved scissors (Fig. 2A). The bottom flange of the dome was then placed under the skin (Fig. 2B). Buprenorphine was administered intraperitoneally at 0.05 mg/kg for pain relief. This administration was done prior to cell seeding so that the animal would not have to be turned supine after cell seeding. On the day of cell seeding, cells were thawed in a 37 °C water bath and were transferred to 10 mL of complete media to rinse off the DMSO. The cells were then re-



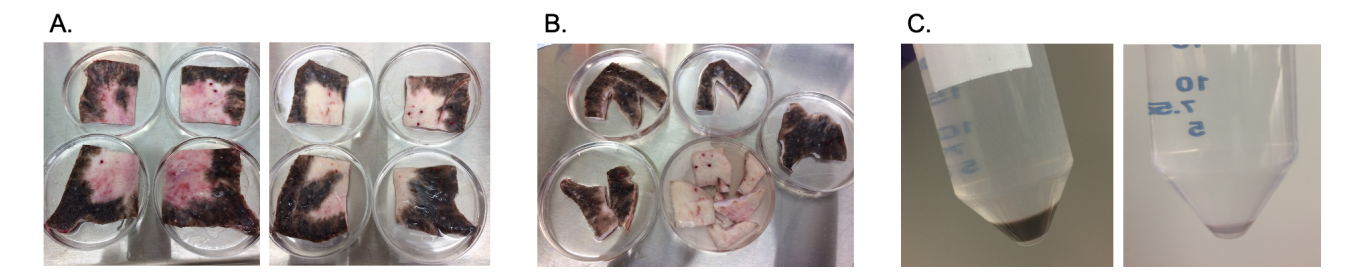


Fig. 1. Dyspigmented epidermal cells are isolated from porcine HTS as shown. Scars are excised on the terminal experimental day (A). Scars are cut into pigmentation phenotypes and sorted (B). Scars are further cut and treated with dispase to isolate epidermal cells (C) which were cryopreserved until use in the xenograft model. HTS, hypertrophic scar.

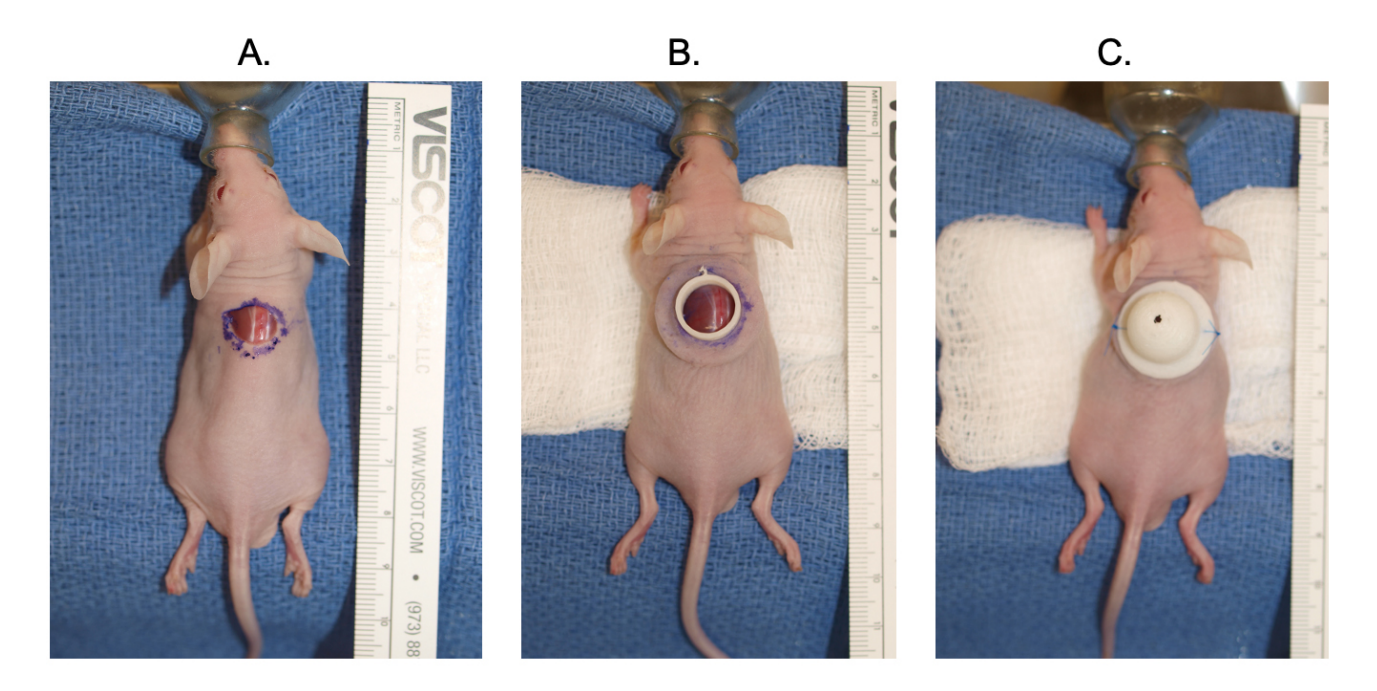


Fig. 2. The dome placement and cell seeding xenografting procedure is detailed. A full thickness excision is performed on the dorsum of the mouse (A). The bottom flange is placed (B). The cells are seeded, and the top dome is secured with suture on either side (C).

suspended in complete media and counted. 8e6 fibroblast cells were re-suspended in 50 μ L of a mixture of 50% Matrigel (Corning) and 50% Cnt-40 media (CellnTec). An iteration of the procedure where the cells were reconstituted in 500 μ L of media was also performed and deemed to be far inferior to 50 μ L. Additionally, normal cell media without Matrigel was attempted, however there were problems with cell leakage, and thus that method was discontinued. Likewise, the problem of leakage was attempted to be controlled with medical grade glue (Dermabond, Ethicon, Raritan, Franklin Township, NJ, USA) and with commercially available superglue, but these methods were toxic to cells and did not result in the creation of a robust xenograft.

The suspension was aliquoted onto the open wound area with care taken to hold the flange in place to prevent leakage while the gel formed (Matrigel forms a gel after heating to 37 °C). After 60 seconds, the top portion of the

dome was put into place over the flange such that the mouse skin was sandwiched between the top of the dome and the flange. Two 5-O proline sutures were then tied onto opposite sides of the dome to prevent it from moving (Fig. 2C). The animal was allowed to recover on heat and returned to normal housing once normal movement was observed.

2.3.3 Epidermal Cell Seeding

On day 3, animals were anesthetized as described above and maintained on isoflurane via nose cone. The right suture was removed, and the top portion of the dome was moved to the side. On the day of cell seeding, cells were thawed in a 37 °C water bath and were transferred to 10 mL of complete media to rinse off the DMSO. The cells were then re-suspended in complete media and counted. 1-2e6 epidermal cells were re-suspended and seeded in 50 μL of a mixture of 50% Matrigel and 50% Cnt-40 media as



Table 1. Optimization of porcine xenograft in nude mouse model and treatment dosages and timing.

Group	Dermal Cell Type	Epidermal Cell Type		
1	NPDF	NPE		
2	HTSDF (P)	Hyper-PE		
3	HTSDF (P)	Hypo-PE		
4	NPDF	NPE		
5	NPDF	NPE		
6	HTSDF (P)	Hypo-PE		
7	HTSDF (P)	Hypo-PE		
8	HTSDF (P)	Hypo-PE		

Abbreviations: NPDF, Normal porcine dermal fibroblasts; NPE, normal porcine epidermal cells; HTSDF (P), Hypertrophic scar dermal fibroblasts-porcine; Hyper-PE, Hyper-pigmented porcine epidermal cells; Hypo-PE, Hypo-pigmented porcine epidermal cells.

described above. The dome was then re-sutured in place and the animal was allowed to recover. An iteration of the model where fibroblasts and epidermal cells were seeded on the same day was attempted and resulted in primarily dermis generation with minimal epidermis, and hence was not pursued. This ratio of cells was determined empirically from our other published grafting studies. Assuming a human basal keratinocyte ranges from 20 to 40 µm² in vivo, and the hole in the grafting flange is 1 cm diameter = $3.14 (0.5 \text{ cm})^2 = 0.78 \text{ cm}^2$, the basal cell area of the wound would fit $(7.8 \times 10^{-1})/(2 \times 10^{-7}) = 3.9 \times 10^6$ cells. 5 million input cells is therefore roughly the amount needed for engraftment, followed by proliferation to generate all the stratified epithelial layers. The average number of fibroblasts in a human biopsy, as determined by a trypsin EDTA digestion is 4.0×10^6 cells/cm² [38]; a 2-fold greater concentration was added for our xenografts. Other estimates differ based on technique used, such as a stereotypic measurement [39], or isolation and measurements of viability, which yields $73,952 \pm 19,426/\text{mm}^2$ for epidermal cells, or 7.4×10^6 /cm², which is close to the amount that was added in this study [40].

2.3.4 Dome Removal

On day 7, the animals were anesthetized as described above and maintained on isoflurane via nose cone. The top of the dome was removed and discarded. The bottom flange was carefully removed, using a scalpel is necessary, with care taken not to disturb the fragile xenograft layer. The xenograft was photographed and covered with an occlusive Tegaderm dressing (Cardinal Health, Dublin, OH, USA) and the dressing was sutured in place at multiple contact points to prevent the animal from tampering with the xenograft (Fig. 3).

2.3.5 Sample Collection and Processing

On day 14, the animals were anesthetized as described above and maintained on isoflurane via nose cone. A necropsy was carried out and exsanguination was per-

formed via cardiac stick. Once death was confirmed, the xenograft was excised and tied into a histology cassette to maintain the xenograft orientation. The cassette was then put into 10% neutral buffered formalin for fixation. Following fixation, the xenograft was paraffin-embedded, sectioned, and stained with H&E.

2.3.6 Optimization of Treatment Parameters

A number of different cell types (hyper-, hypo-, and normally pigmented scar and skin) and treatment parameters were tested throughout the course of the model development. Xenograft were successfully created using normallypigmented epidermal cells and normal porcine dermal fibroblasts (NPDF) (Table 1, Group 1). Subsequently, hyperpigmented (Table 1, Group 2) and hypo-pigmented (Table 1, Group 3) xenografts were also successfully created. Once xenografts were successfully created, normal porcine epidermal cells were used to test treatments. A dosage of 10 μ M NDP α -MSH was chosen as an initial starting point for treatment based on the dose applied in vitro to cells. This dose was given as a treatment on day 7 and day 10. Punch biopsies were collected on day 10 and used for molecular analysis by quantitative real-time polymerase chain reaction (qRT-PCR). Additional samples were collected on day 14. This group of animals indicated that there was a slight increase in melanogenesis gene expression at day 10, however, it was not significant (Table 1, Group 4). Finally, a dosage of 100 μ M NDP α -MSH was delivered on day 7 and the samples were collected on day 10 (Table 1, Group 5) (Fig. 3). A significant response was seen in the normally pigmented epidermal cells, and therefore, the remainder of the groups used this treatment were hypo-pigmented epidermal cells (Table 1, Groups 6–8) (Table 2). The different groups were used to collect samples intended for different assays. The optimized parameters and treatment metrics are detailed in Table 2.

2.3.7 Treatment with NDP α -MSH

A subset of animals with either normally-pigmented (n = 3) or hypo-pigmented (n = 9) epidermal cells and HTS-DFs were treated with NDP $\alpha\text{-MSH}.$ On day 7, channels were created in the xenograft with a microneedler with 1.5 mm needles (Petunia Skincare). 50 μL of 100 μM NDP $\alpha\text{-MSH}$ was applied. Tegaderm dressing was applied after 60 seconds to allow for the liquid to penetrate the skin before application. Samples were collected on day 10. 2 mm punch biopsies were collected and were formalin-fixed and paraffin-embedded. The remainder of the xenograft was stored for molecular work.

2.3.8 Sample Processing and Gene and Protein Expression Analysis

From the formalin fixed paraffin embedded (FFPE) samples, sections were created and stained using H&E. Images were obtained to qualitatively characterize skin and scar xenograft structure and epidermal thickness.



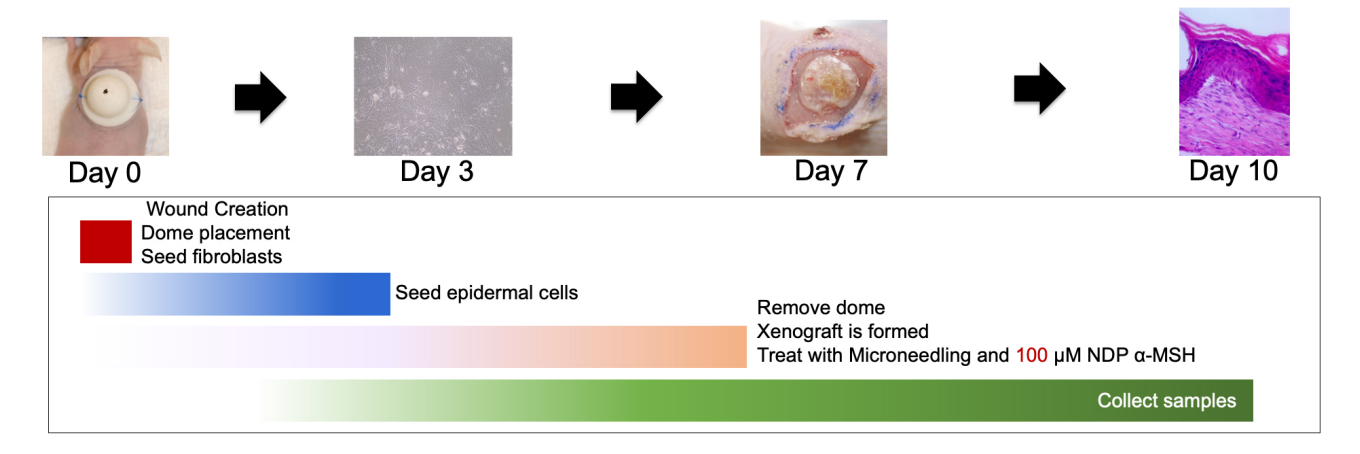


Fig. 3. The xenografting procedure including dome removal, treatment, and sample collection is detailed. NDP α -MSH, synthetic alpha melanocyte stimulating hormone.

Table 2. Animal Groups with the specified treatments and type of sample collected.

Group	Treatment	# of animals (sham/treatment)	Type of Sample Collected	Variable optimized or experiment performed
1	Day 7: 100 μ M NDP α -MSH + microneedling	3 sham/3 treatment	Day 10: Molecular preservation Punch bx for FFPE	Treatment effect on normal cells?
2	Day 7: 100 μ M NDP α -MSH + microneedling	3 sham/3 treatment	Day 10: Molecular preservation Punch bx for FFPE	Treatment effect on hypo-pigmented cells? Type of sample collected.
3	Day 7: 100 μ M NDP α -MSH + microneedling	3 sham/3 treatment	Day 10: Molecular preservation Punch bx for FFPE	Treatment effect on hypo-pigmented cells? Type of sample collected.
4	Day 7: 100 μ M NDP α -MSH + microneedling	3 sham/3 treatment	Day 10: Molecular preservation Punch bx for FFPE	Treatment effect on hypo-pigmented cells? Type of sample collected.

FFPE, formalin fixed paraffin embedded.

From the samples preserved for molecular work, the RNeasy fibrous tissue kit was used to isolate and quantify mRNA from the xenografts. Melanin was also isolated from a group of tissues as previously described [41]. In brief, the pellet was dissolved in 1 N NaOH, incubated for 30 minutes at 100 °C, and melanin was measured by absorbance at 405 nm normalized to a standard curve with synthetic melanin (Sigma Aldrich, Burlington, MA, USA).

100 ng of RNA at a concentration of 10 ng/ μ L of mRNA was incubated with primers, reverse transcriptase, and SYBR green. An increased amount of template mRNA had to be used due to the low percentage of the xenograft that makes up the epidermis, and the relatively low proportion of the epidermis that consists of melanocytes. An iteration of this protocol was run with 10 ng of total mRNA and the C_t values were too low to interpret. Primers to TYR, TYRP1, DCT, and GAPDH are previously described [37]. The $\Delta\Delta C_t$ method was used with the untreated shams serving as the control and GAPDH as the housekeeping gene.

Protein was isolated from the molecularly-preserved xenografts using RIPA buffer with 10 μL/mL of protease inhibitor cocktail (Sigma Aldrich). A mortar and pestle was used to grind tissue in 1mL of RIPA buffer. The subsequent homogenate was sonicated (ThermoFisher Scientific, Waltham, MA, USA) with 5 pulses (1 sec pulse, 6 second pulse delay), then spun at 10,000 g for 10 minutes. The supernatant was saved and protein was quantified using a Bradford assay. Eighty mg of heated-denatured total protein per sample was subjected to Sodium dodecylsulfate polyacrylamide gel electrophoresis (SDS-PAGE) using 10% precast (Biorad) gels, along with precision plus protein western C ladder (Biorad). The proteins were transferred to a nitrocellulose membrane (Biorad, Hercules, CA, USA) and blocked for 3 hours with 3% non-fat dry milk. The primary antibody for TYRP1 (ab83774 at 1 µg/mL) was applied for overnight incubation. The membrane was rinsed with TBST, then the secondary antibody which was a goat-anti rabbit HRP-cinjugated antibody was applied at 1:10,000. The blot was then developed with Super-



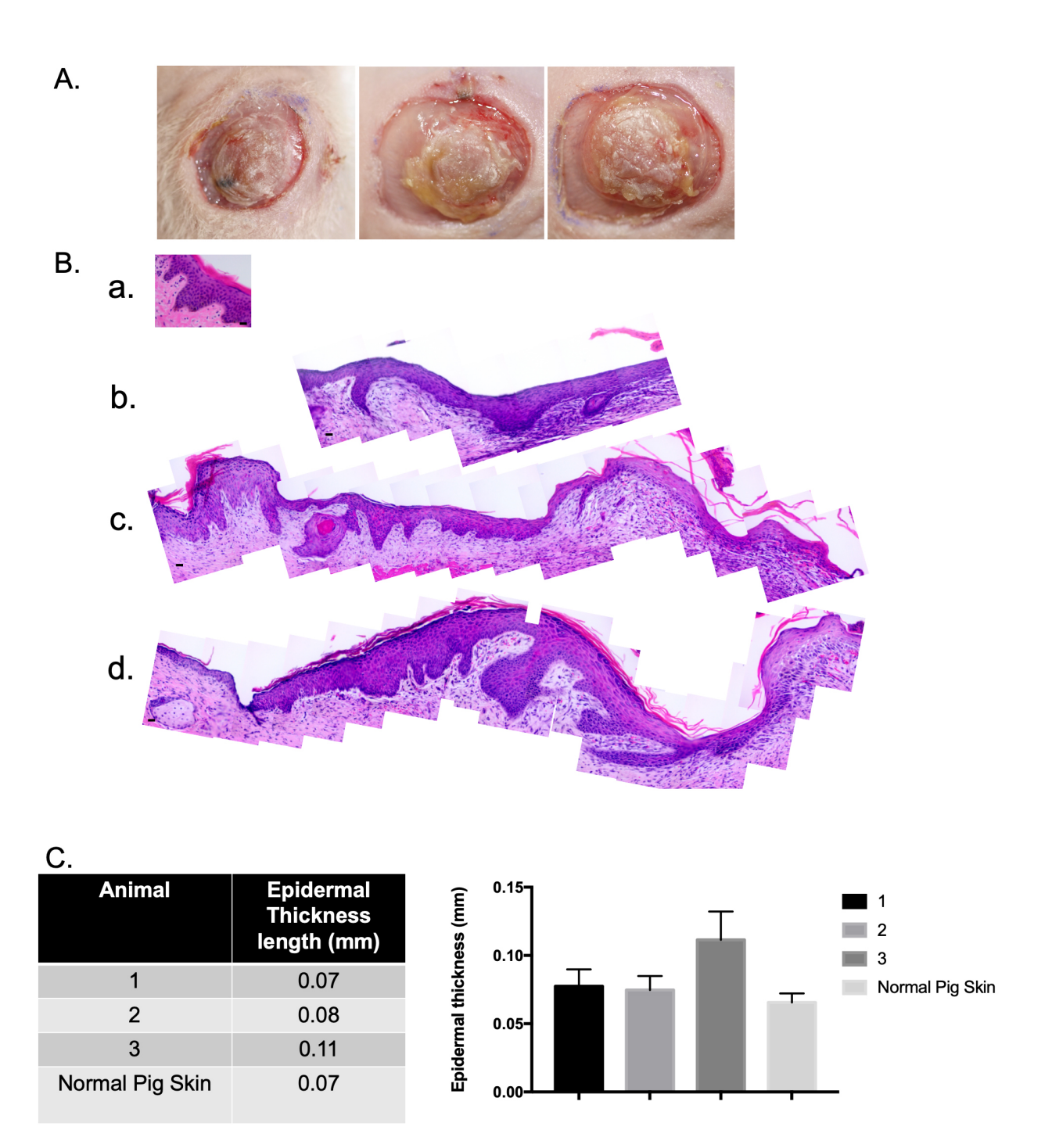


Fig. 4. Normally pigmented skin epidermal cells and normal porcine dermal fibroblasts were used to create a xenograft that is histologically similar to uninjured pig skin. Macroscopic images of xenografts at day 10 (A). Punch biopsies of the xenografts were taken at day 14 and were FFPE and stained with hematoxylin and eosin (H&E). Microscopic images of H&E-stained xenograft sections (B). Un-injured porcine skin (a). Animal 1 (b). Animal 2 (c). Animal 3 (d). N = 3. Epidermal thickness was measured using ImageJ (C). (Scale bar = 20 μ m) (mean \pm standard error of the mean (SEM), n = 10 technical replicates).

Signal West Dura substrate (ThermoFisher Scientific) and imaged with chemiluminescent imaging (Cytiva Life Sciences, Marlborough, MA, USA). Bands were quantified by densitometry analysis. Protein expression levels are divided by GAPDH to normalized to varying levels determined by densitometry, then plotted.

3. Results

3.1 Normally-Pigmented Porcine Skin Cells can be Used to Generated Porcine Xenografts in Nude Mice

After the optimization of printing of domes, seeding volume, and cell leakage (Table 1), normally pigmented porcine epidermal cells and normal porcine dermal



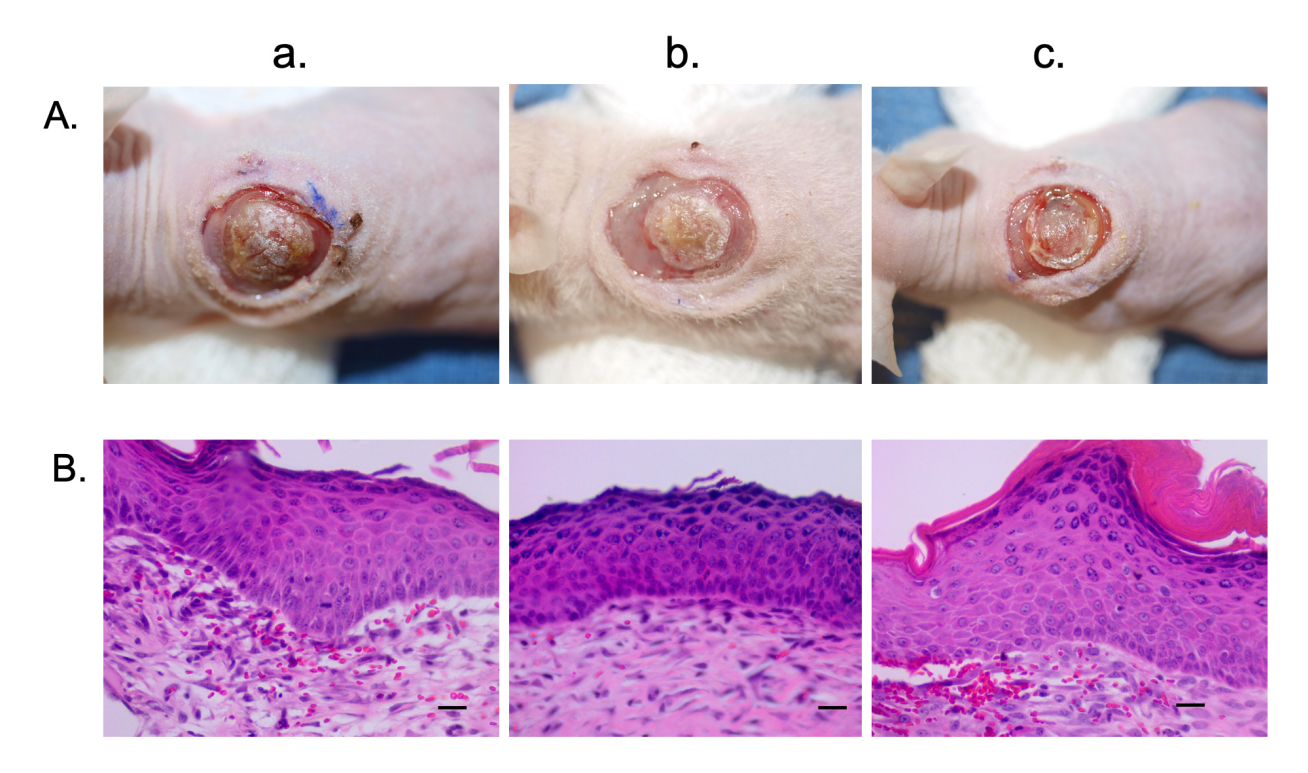


Fig. 5. Hyper-pigmented scar epidermal cells and HTS dermal fibroblasts were used to create a xenograft that is histologically similar to hyper-pigmented pig scar. Macroscopic images of xenografts at day 10 (A). Punch biopsies of the xenografts were taken at day 14 and were FFPE and stained with H&E. Microscopic images of H&E-stained xenograft sections (B). Animal 1 (a). Animal 2 (b). Animal 3 (c). N = 3 (bottom) (Scale bar = 20 μ m).

fibroblasts were used to create xenografts. The xenografts were imaged at day 10 (Fig. 4A). Samples were collected on day 14 and were FFPE and stained with H&E. The xenografts contain an epidermis and a dermis, and the epidermis looked similar to uninjured pig skin (Fig. 4B) with the presence of epidermal rete ridges and associated dermal papillae. When these different samples were measured using ImageJ (Version 1.53a, National Institutes of Health, Bethesda, MD, USA), it was concluded that a stratified epidermis in similar thickness to uninjured pig skin was created (Fig. 4C). The xenograft was $0.11 \pm 0.07~\mu m~vs.~0.06 \pm 0.03~\mu m$ in normal pig skin, a difference that was not significant.

3.2 Hyper- and Hypo-Pigmented Scar Cells can be Used to Generate Porcine Xenografts in Nude Mice

This model was also tested using hyper-pigmented scar epidermal cells. These cells resulted in similar xenografts to the normally pigmented xenografts (Fig. 5A). The histo-architecture of these xenografts revealed a xenograft similar in structure to hyper-pigmented scar in the pig model. There were few rete ridges, and the epidermis was thicker compared to the normally pigmented skin xenograft (Fig. 5B).

Last, the model was tested using hypo-pigmented scar epidermal cells. These cells resulted in very similar xenografts at the gross (Fig. 6A) and histologic level (Fig. 6B).

3.3 Normally Pigmented Xenografts can be Stimulated to Produce Melanin by Synthetic α -MSH in Vivo

Normally pigmented xenografts were treated with microneedling and a 100 μ M topical application of NDP α -MSH, and samples were collected at day 10, 3 days after treatment (Fig. 7). Samples were saved for molecular analysis of the tissues and qRT-PCR was performed for TYR, TYPR1, and DCT. In the treated group, there was upregulation of TYR (4.4 \pm 2.3 vs. -0.3 ± 1.1), TYRP1 (1.37 \pm 0.27 vs. 0.33 \pm 0.78), and DCT (2.54 \pm 2.54 vs. $-0.3 \pm$ 0.95) compared to the untreated controls (n = 3) (Fig. 7).

3.4 Hypo-Pigmented Xenografts can be Stimulated to Produce Melanin by Synthetic α -MSH in Vivo

Hypo-pigmented xenografts were treated as above, and samples were collected at day 10 for molecular analysis of melanin levels (Fig. 8A). Treated xenografts had 5.43 ± 1.41 mg of melanin/g of tissue, while controls had 1.55 ± 0.74 . (Fig. 8B). In a separate group, treated in the same manner, qRT-PCR was performed for TYR, TYPRI, and DCT. In the treated group, there was up-regulation of TYR (2.7 \pm 1.1 vs. 0.3 \pm 1.1), TYRPI (2.6 \pm 0.6 vs. 0.3 \pm 0.7), and DCT (0.7 \pm 0.9 vs. 0.3 \pm 1) fold change from control (n = 3) (Fig. 8C). In another group, there was increased protein expression of TYRP1 in the treated samples compared to the control (0.71 \pm 0.36 vs. 0.47 \pm 0.51) (Fig. 8D).



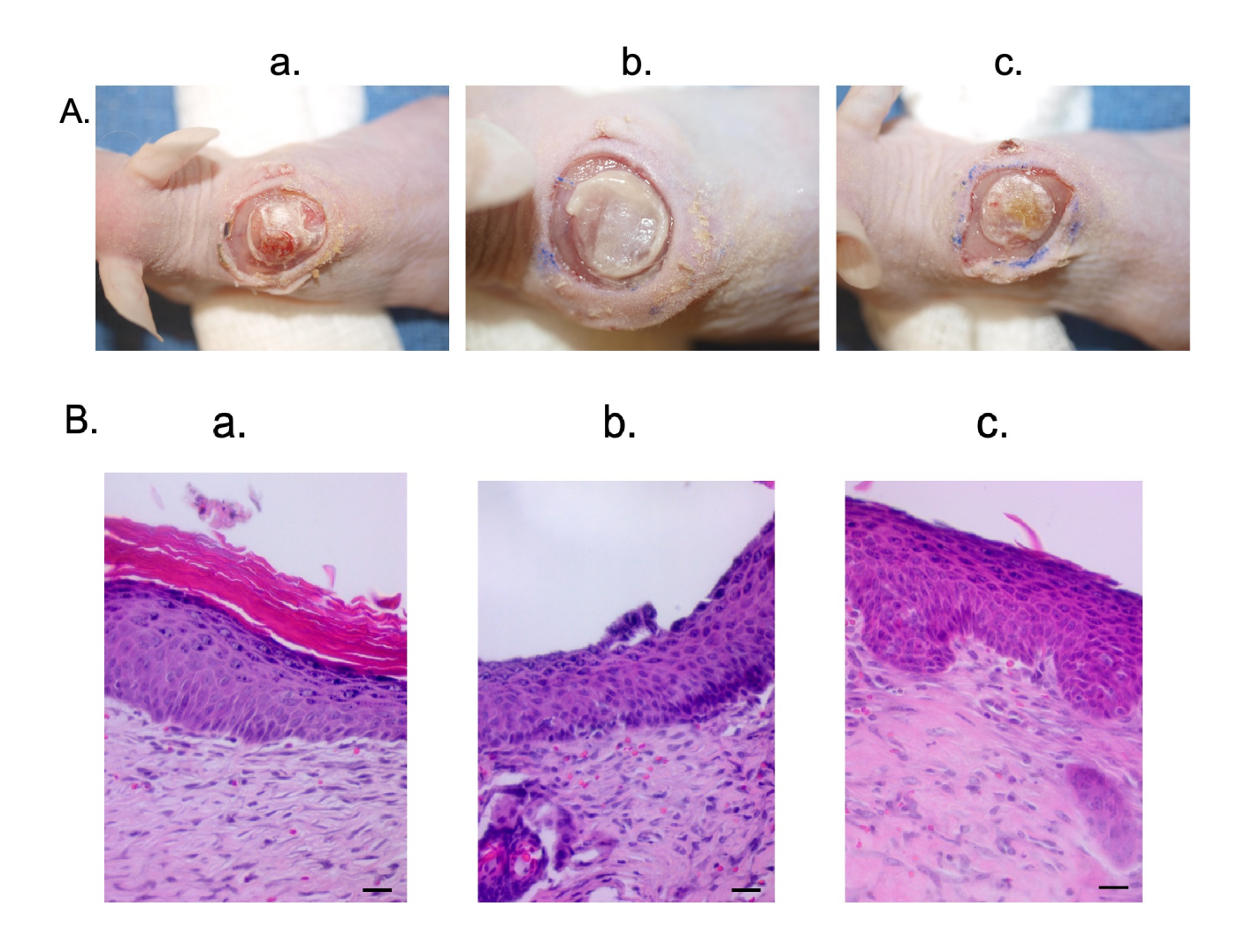


Fig. 6. Hypo-pigmented scar epidermal cells and HTS dermal fibroblasts were used to create a xenograft that is histologically similar to hypo-pigmented pig scar. Macroscopic images of xenografts at day 10 (A). Punch biopsies of the xenografts were taken at day 14 and were FFPE and stained with H&E. Microscopic images of H&E-stained xenograft sections (B). Animal 1 (a). Animal 2 (b). Animal 3 (c). N = 3 (bottom) (Scale bar = 20 μ m).

4. Discussion

A nude mouse xenograft model is suitable for studying HTS *in vivo*. The seeding of normal fibroblasts and normally-pigmented epidermal cells created a full thickness skin equivalent that contained an epidermis and dermis. This structure was similar to normal skin in its approximation of rete ridges. The presence of melanocytes in this skin structure was confirmed when the normally-pigmented xenografts were treated with synthetic NDP α -MSH. There was up-regulated gene transcription of the 3 genes required for melanin synthesis after treatment. Melanocytes are the only cell type that have this pigmentation machinery; thus, the cell type was present. In addition, the primers that were used are specific and unique to porcine sequences, and thus, the xenograft tissues were composed of porcine cells, not mouse cells.

HTS fibroblasts and hyper- and hypo-pigmented epidermal cells also created full thickness skin with a stratified epithelium. These skin structures likewise contained melanocytes of pig origin for the reasons described above. The use of microneedling to create channels in the skin through which the topical application of the drug could be delivered was a success in this model. One of the reasons why it needed to be tested *in vivo* was to test if this treatment could work to penetrate the epidermis and cause a response in melanocytes. This work confirms that hypo-pigmented melanocytes do not lose the ability to make melanin. They are simply in a state of non-pigment production, and can be signaled to synthesize melanin with synthetic NDP α -MSH.

While we have previously xenografted primary human skin cells, patient-derived dyschromic HTS can only be derived in smaller amounts, within a limited time-frame, and only after healing. Additionally, patient HTS are most likely at the severe end of the spectrum because samples large enough to graft can most often only be collected from severe HTS that requires excision. Human wound stud-





Fig. 7. Normally pigmented skin xenografts treated with microneedling and NDP α -MSH had TYR, TYRP1, and DCT gene expression up-regulation compared to controls. Macroscopic images of xenografts at day 10 (A). Animal 1 (a). Animal 2 (b). RNA isolated was isolated from xenografts and subjected to quantitative real-time polymerase chain reaction (qRT-PCR) for TYR, TYRP1, and DCT. GAPDH was used as a housekeeping control (mean \pm SEM, n = 3 xenografts/group) (B). Differences are not significant.

ies are also limited by heterogeneity of the patients, wound types, and cells within the wound. Finally, HTS-prone patients are generally not included as a resource for preclinical studies because of the potential for worsening of scars.

There are several limitations to this model. One limitation is that, although the xenografts resemble skin upon histological examination, the xenografts do not entirely re-

semble normal porcine skin upon visual inspection. Although this is true, skin was deduced to be present when, 5–10 minutes after dome removal on day 7, the cells dried and the cornified layer typical of keratinocytes could be easily viewed (**Supplementary Fig. 1**). Another limitation is that the melanin that was made through transcription of TYR, TYPR1, and DCT could not be readily seen



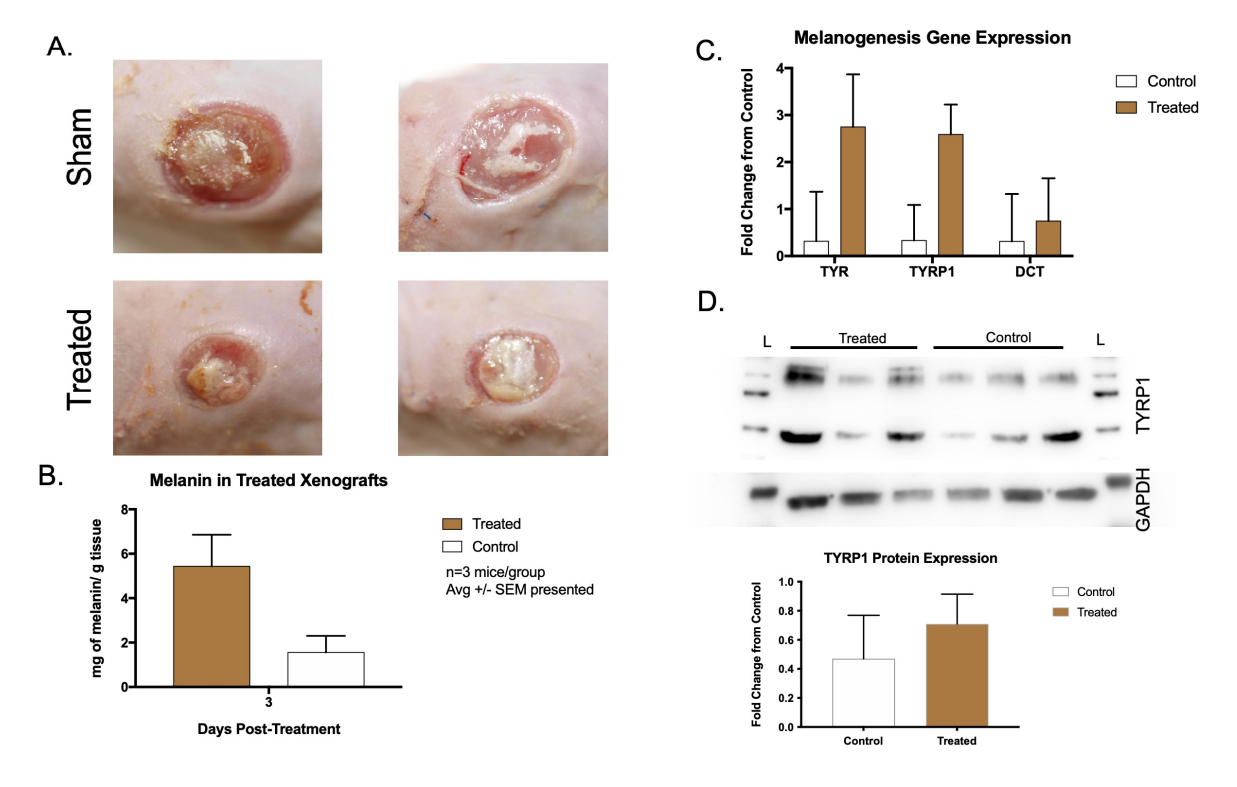


Fig. 8. Hypo-pigmented scar xenografts treated with microneedling and NDP α -MSH had TYR, TYRP1, and DCT gene expression and melanin up-regulation compared to controls. Macroscopic images of xenografts at day 10 (A). Melanin (B) and RNA (C) were isolated from xenografts and RNA was subjected to qRT-PCR for TYR, TYRP1, and DCT (n = 3). GAPDH was used as a housekeeping control (mean \pm SEM, n = 3 xenografts/group). Differences are not significant. Protein was isolated and immunoblot analysis was performed for TYRP1 expression (D).

upon gross examination of the xenografts. This could be due to a loss of melanin after melanocyte production. Another possibility is that melanin levels did not reach those that could be detected by visual inspection. The advantage to this model is that it allowed for the confirmation of the hypothesis that hypo-pigmented cells could be stimulated to produce melanin related genes. Melanin was also detected using biochemical methods. However, future work will be aimed at using this treatment in the Duroc pig model. Another limitation of the xenograft model is the absence of professional immune cells, although human T cells have been used in xenografts in the study of psoriasis and other skin disorders. Clearly, the immune system plays an important role in hemostasis, wound healing, and scar formation. While the pathophysiological role of the immune system in HTS dyschromia has not been fully elucidated [42], proinflammatory cytokines, as well as reactive oxygen species, secreted in response to burns and other wounds may alter melanocyte proliferation and differentiation [43–46].

This xenograft animal model can be used to study topical treatments for any skin condition. Cells from adult patients can be isolated, grown in culture, and seeded to make xenografts. Possible topic areas for study are systemic sclerosis, psoriasis, discoid lupus, or post-inflammatory hyperor hypo-pigmentation. These xenografts could also be useful for topical drug delivery studies. In addition, differ-

ent cell phenotypes can be mixed and matched using this model to study paracrine cell signaling. For example, normal fibroblasts could be mixed with pathogenic epidermal cells or *vice versa*. Finally, this model may have some advantages over direct testing of topical therapeutics in pig models because once promising compounds/techniques are studied in the xenograft mouse model, we can then go back from mouse xenograft to pigs with fewer animals yielding lower costs and more streamlined and time-efficient drug development processes.

We have also employed 3D cell culture models [47], derived either commercially (EpiDerm, MatTek) or within our lab, and found them to be invaluable for some applications [48]. In our hands, we found the xenograft model provides more reliable graft takes, especially with a 3-cell model (keratinocytes, fibroblasts, and melanocytes) than those from 3D cell culture models. The xenografts demonstrate longer survival of all three cell types, robust proliferation, and recapitulate epidermal biochemical and morphological differentiation. Further, the xenograft model works with or without cell immortalization or reprogramming, and works with adult and neonatally-derived skin cells. For these reasons, we have used it as a model for testing nonmurine skin cells for its response to DNA alkylation [49], jet fuel toxicity [50], melanoma-melanocyte differentiation [32], sulfur mustard [29] and UVB-induced apoptosis. We



find that the technique is easily learned, and completion time is similar to that of 3D histiotypic or organotypic culture models.

5. Conclusions

Adult skin cells can be xenografted onto nude mice to create a skin construct with epidermal and dermal layers that is responsive to pigmentation agonists. The skin constructs contain stratified epithelia and can be treated topically and through microneedling-assisted drug delivery.

Availability of Data and Materials

Datasets are available upon reasonable request of the corresponding author.

Author Contributions

BCC, CMSR, DSR, JWS designed the research study. BCC performed the research. BCC analyzed the data. BCC wrote the manuscript. All authors contributed to editorial changes in the manuscript. All authors read and approved the final manuscript. All authors have participated sufficiently in the work and agreed to be accountable for all aspects of the work.

Ethics Approval and Consent to Participate

All animal work was approved by the MedStar Health Research Institute's Institutional Animal Care and Use Committee (No. 2001000190 or 2018-001).

Acknowledgment

The authors acknowledge Nicholas J. Prindeze, MD for 3D printing the domes used in this work.

Funding

This research received no external funding.

Conflict of Interest

The authors declare no conflict of interest.

Supplementary Material

Supplementary material associated with this article can be found, in the online version, at https://doi.org/10.31083/j.fbl2906230.

References

- [1] Ramos MLC, Gragnani A, Ferreira LM. Is there an ideal animal model to study hypertrophic scarring? Journal of Burn Care & Research: Official Publication of the American Burn Association. 2008; 29: 363–368.
- [2] Domergue S, Jorgensen C, Noël D. Advances in Research in Animal Models of Burn-Related Hypertrophic Scarring. Journal of Burn Care & Research: Official Publication of the American Burn Association. 2015; 36: e259–e266.
- [3] Abdullahi A, Amini-Nik S, Jeschke MG. Animal models in burn research. Cellular and Molecular Life Sciences: CMLS. 2014; 71: 3241–3255.

- [4] Ud-Din S, Bayat A. Non-animal models of wound healing in cutaneous repair: *In silico*, in vitro, ex vivo, and in vivo models of wounds and scars in human skin. Wound Repair and Regeneration. 2017; 25: 164–176.
- [5] Wang J, Ding J, Jiao H, Honardoust D, Momtazi M, Shankowsky HA, et al. Human hypertrophic scar-like nude mouse model: characterization of the molecular and cellular biology of the scar process. Wound Repair and Regeneration. 2011; 19: 274–285.
- [6] Honardoust D, Kwan P, Momtazi M, Ding J, Tredget EE. Novel methods for the investigation of human hypertrophic scarring and other dermal fibrosis. Methods in Molecular Biology (Clifton, N.J.). 2013; 1037: 203–231.
- [7] Momtazi M, Kwan P, Ding J, Anderson CC, Honardoust D, Goekjian S, et al. A nude mouse model of hypertrophic scar shows morphologic and histologic characteristics of human hypertrophic scar. Wound Repair and Regeneration. 2013; 21:77– 87
- [8] Alrobaiea SM, Ding J, Ma Z, Tredget EE. A Novel Nude Mouse Model of Hypertrophic Scarring Using Scratched Full Thickness Human Skin Grafts. Advances in Wound Care. 2016; 5: 299– 313
- [9] Carney BC, Travis TE, Moffatt LT, Johnson LS, McLawhorn MM, Simbulan-Rosenthal CM, et al. Hypopigmented burn hypertrophic scar contains melanocytes that can be signaled to repigment by synthetic alpha-melanocyte stimulating hormone in vitro. PloS One. 2021; 16: e0248985.
- [10] Dorr RT, Ertl G, Levine N, Brooks C, Bangert JL, Powell MB, et al. Effects of a superpotent melanotropic peptide in combination with solar UV radiation on tanning of the skin in human volunteers. Archives of Dermatology. 2004; 140: 827–835.
- [11] Dorr RT, Dvorakova K, Brooks C, Lines R, Levine N, Schram K, et al. Increased eumelanin expression and tanning is induced by a superpotent melanotropin [Nle4-D-Phe7]-alpha-MSH in humans. Photochem Photobiol. 2000; 72: 526–532.
- [12] Levine N, Sheftel SN, Eytan T, Dorr RT, Hadley ME, Weinrach JC, et al. Induction of skin tanning by subcutaneous administration of a potent synthetic melanotropin. JAMA. 1991; 266: 2730–2736.
- [13] Barnetson RS, Ooi TK, Zhuang L, Halliday GM, Reid CM, Walker PC, et al. [Nle4-D-Phe7]-alpha-melanocyte-stimulating hormone significantly increased pigmentation and decreased UV damage in fair-skinned Caucasian volunteers. The Journal of Investigative Dermatology. 2006; 126: 1869–1878.
- [14] Lim HW, Grimes PE, Agbai O, Hamzavi I, Henderson M, Haddican M, et al. Afamelanotide and narrowband UV-B phototherapy for the treatment of vitiligo: a randomized multicenter trial. JAMA Dermatology. 2015; 151: 42–50.
- [15] Grimes PE, Hamzavi I, Lebwohl M, Ortonne JP, Lim HW. The efficacy of afamelanotide and narrowband UV-B phototherapy for repigmentation of vitiligo. JAMA Dermatology. 2013; 149: 68–73.
- [16] Harms J, Lautenschlager S, Minder CE, Minder EI. An alphamelanocyte-stimulating hormone analogue in erythropoietic protoporphyria. The New England Journal of Medicine. 2009; 360: 306–307.
- [17] Biolcati G, Marchesini E, Sorge F, Barbieri L, Schneider-Yin X, Minder EI. Long-term observational study of afamelanotide in 115 patients with erythropoietic protoporphyria. The British Journal of Dermatology. 2015; 172: 1601–1612.
- [18] Harms JH, Lautenschlager S, Minder CE, Minder EI. Mitigating photosensitivity of erythropoietic protoporphyria patients by an agonistic analog of alpha-melanocyte stimulating hormone. Photochemistry and Photobiology. 2009; 85: 1434–1439.
- [19] Hadley ME, Wood SH, Lemus-Wilson AM, Dawson BV, Levine N, Dorr RT, et al. Topical application of a melanotropic peptide



- induces systemic follicular melanogenesis. Life Sciences. 1987; 40: 1889–1895.
- [20] Dorr RT, Dawson BV, al-Obeidi F, Hadley ME, Levine N, Hruby VJ. Toxicologic studies of a superpotent alphamelanotropin, [Nle4, D-Phe7]alpha-MSH. Investigational New Drugs. 1988; 6: 251–258.
- [21] Erlendsson AM, Anderson RR, Manstein D, Waibel JS. Developing technology: ablative fractional lasers enhance topical drug delivery. Dermatologic Surgery. 2014; 40: S142–S146.
- [22] Alkilani AZ, McCrudden MTC, Donnelly RF. Transdermal Drug Delivery: Innovative Pharmaceutical Developments Based on Disruption of the Barrier Properties of the stratum corneum. Pharmaceutics. 2015; 7: 438–470.
- [23] Haedersdal M, Erlendsson AM, Paasch U, Anderson RR. Translational medicine in the field of ablative fractional laser (AFXL)assisted drug delivery: A critical review from basics to current clinical status. Journal of the American Academy of Dermatology. 2016; 74: 981–1004.
- [24] Waibel JS, Rudnick A, Shagalov DR, Nicolazzo DM. Update of Ablative Fractionated Lasers to Enhance Cutaneous Topical Drug Delivery. Advances in Therapy. 2017; 34: 1840–1849.
- [25] Sivamani RK, Liepmann D, Maibach HI. Microneedles and transdermal applications. Expert Opinion on Drug Delivery. 2007; 4: 19–25.
- [26] Hao Y, Li W, Zhou X, Yang F, Qian Z. Microneedles-Based Transdermal Drug Delivery Systems: A Review. Journal of Biomedical Nanotechnology. 2017; 13: 1581–1597.
- [27] Alster TS, Graham PM. Microneedling: A Review and Practical Guide. Dermatologic Surgery. 2018; 44: 397–404.
- [28] Salgado G, Ng YZ, Koh LF, Goh CSM, Common JE. Human reconstructed skin xenografts on mice to model skin physiology. Differentiation; Research in Biological Diversity. 2017; 98: 14– 24
- [29] Rosenthal DS, Velena A, Chou FP, Schlegel R, Ray R, Benton B, et al. Expression of dominant-negative Fas-associated death domain blocks human keratinocyte apoptosis and vesication induced by sulfur mustard. The Journal of Biological Chemistry. 2003; 278: 8531–8540.
- [30] Trabosh VA, Divito KA, D Aguda B, Simbulan-Rosenthal CM, Rosenthal DS. Sequestration of E12/E47 and suppression of p27KIP1 play a role in Id2-induced proliferation and tumorigenesis. Carcinogenesis. 2009; 30: 1252–1259.
- [31] Lichti U, Anders J, Yuspa SH. Isolation and short-term culture of primary keratinocytes, hair follicle populations and dermal cells from newborn mice and keratinocytes from adult mice for in vitro analysis and for grafting to immunodeficient mice. Nature Protocols. 2008; 3: 799–810.
- [32] DiVito KA, Trabosh VA, Chen YS, Chen Y, Albanese C, Javelaud D, et al. Smad7 restricts melanoma invasion by restoring N-cadherin expression and establishing heterotypic cell-cell interactions in vivo. Pigment Cell & Melanoma Research. 2010; 23: 795–808.
- [33] Carney BC, Dougherty RD, Moffatt LT, Simbulan-Rosenthal CM, Shupp JW, Rosenthal DS. Promoter Methylation Status in Pro-opiomelanocortin Does Not Contribute to Dyspigmentation in Hypertrophic Scar. Journal of Burn Care & Research: Official Publication of the American Burn Association. 2020; 41: 339–346.
- [34] Carney BC, Chen JH, Kent RA, Rummani M, Alkhalil A, Moffatt LT, et al. Reactive Oxygen Species Scavenging Potential Contributes to Hypertrophic Scar Formation. The Journal of Surgical Research. 2019; 244: 312–323.
- [35] Alkhalil A, Carney BC, Travis TE, Muhie S, Miller SA, Ramella-Roman JC, et al. Dyspigmented hypertrophic scars: Beyond skin color. Pigment Cell & Melanoma Research. 2019; 32: 643–656.

- [36] Mino MJ, Mauskar NA, Matt SE, Pavlovich AR, Prindeze NJ, Moffatt LT, *et al.* A fitted neoprene garment to cover dressings in swine models. Lab Animal. 2012; 42: 23–25.
- [37] Carney BC, Chen JH, Luker JN, Alkhalil A, Jo DY, Travis TE, et al. Pigmentation Diathesis of Hypertrophic Scar: An Examination of Known Signaling Pathways to Elucidate the Molecular Pathophysiology of Injury-Related Dyschromia. Journal of Burn Care & Research: Official Publication of the American Burn Association. 2019; 40: 58–71.
- [38] Hybbinette S, Boström M, Lindberg K. Enzymatic dissociation of keratinocytes from human skin biopsies for in vitro cell propagation. Experimental Dermatology. 1999; 8: 30–38.
- [39] Bauer J, Bahmer FA, Wörl J, Neuhuber W, Schuler G, Fartasch M. A strikingly constant ratio exists between Langerhans cells and other epidermal cells in human skin. A stereologic study using the optical disector method and the confocal laser scanning microscope. The Journal of Investigative Dermatology. 2001; 116: 313–318.
- [40] Sierra-Sánchez Á, Barbier MA, Magne B, Larouche D, Arias-Santiago S, Germain L. Comparison of Two Human Skin Cell Isolation Protocols and Their Influence on Keratinocyte and Fibroblast Culture. International Journal of Molecular Sciences. 2023; 24: 14712.
- [41] Carney BC, Dougherty RD, Moffatt LT, Simbulan-Rosenthal CM, Shupp JW, Rosenthal DS. Promoter Methylation Status in Pro-opiomelanocortin Does Not Contribute to Dyspigmentation in Hypertrophic Scar. Journal of Burn Care & Research: Official Publication of the American Burn Association. 2020; 41: 339–346.
- [42] Kaufman BP, Aman T, Alexis AF. Postinflammatory Hyperpigmentation: Epidemiology, Clinical Presentation, Pathogenesis and Treatment. American Journal of Clinical Dermatology. 2018; 19: 489–503.
- [43] Taylor S, Grimes P, Lim J, Im S, Lui H. Postinflammatory hyperpigmentation. Journal of Cutaneous Medicine and Surgery. 2009; 13: 183–191.
- [44] Medrano EE, Farooqui JZ, Boissy RE, Boissy YL, Akadiri B, Nordlund JJ. Chronic growth stimulation of human adult melanocytes by inflammatory mediators in vitro: implications for nevus formation and initial steps in melanocyte oncogenesis. Proceedings of the National Academy of Sciences of the United States of America. 1993; 90: 1790–1794.
- [45] Tomita Y, Maeda K, Tagami H. Melanocyte-stimulating properties of arachidonic acid metabolites: possible role in postinflammatory pigmentation. Pigment Cell Research. 1992; 5: 357–361.
- [46] Lacz NL, Vafaie J, Kihiczak NI, Schwartz RA. Postinflammatory hyperpigmentation: a common but troubling condition. International Journal of Dermatology. 2004; 43: 362–365.
- [47] Burks HE, Pokorny JL, Koetsier JL, Roth-Carter QR, Arnette CR, Gerami P, *et al.* Melanoma cells repress Desmoglein 1 in keratinocytes to promote tumor cell migration. The Journal of Cell Biology. 2023; 222: e202212031.
- [48] Rosenthal DS, Kuo LW, Seagrave SL, Soni V, Islam N, Minsky G, et al. Skin Immuno-CometChip in 3D vs. 2D Cultures to Screen Topical Toxins and Skin-Specific Cytochrome Inducers. Genes. 2023; 14: 630.
- [49] Rosenthal DS, Shima TB, Celli G, De Luca LM, Smulson ME. Engineered human skin model using poly(ADP-ribose) polymerase antisense expression shows a reduced response to DNA damage. The Journal of Investigative Dermatology. 1995; 105: 38–43.
- [50] Rosenthal DS, Simbulan-Rosenthal CM, Liu WF, Stoica BA, Smulson ME. Mechanisms of JP-8 jet fuel cell toxicity. II. Induction of necrosis in skin fibroblasts and keratinocytes and modulation of levels of Bcl-2 family members. Toxicology and Applied Pharmacology. 2001; 171: 107–116.

